Sensors & Actuators: A. Physical 378 (2024) 115835

Contents lists available at ScienceDirect

Sensors and Actuators: A. Physical

journal homepage: www.journals.elsevier.com/sensors-and-actuators-a-physical

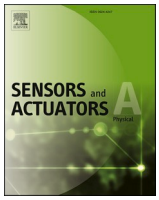

TendrilBot: Modular soft robot with versatile radial grasping and locomotion capabilities

Joshua Knospler, Nicholas Pagliocca, Wei Xue, Mitja Trkov *

Department of Mechanical Engineering, Rowan University, 201 Mullica Hill Rd, Glassboro, NJ 08028, USA

ARTICLE INFO

Keywords:
Soft robots and actuators
Grasping and wrapping
Stiffness modulation
Permanent magnets with coils
Reconfigurable and modular robots
SINDy

ABSTRACT

This paper introduces TendrilBot, a novel modular soft robot designed for versatile manipulation, stiffness modulation, and locomotion tasks. Built upon previously developed modular units, the TendrilBot consists of multiple actuators connected linearly in linear, cylindrical, or helix configurations. Cylindrical configurations (single row or stacked) enable the robot to wrap around objects for grasping and manipulation in a single row or stacked configuration when interconnected with the magnets on sides of the units. Additionally, such configurations further facilitate internal grasping within hollow tubes or objects holding them with its reconfigurable shape. Both wrapping and internal grasping are experimentally validated to demonstrate radial stiffness modulation and squeezing capabilities. By further rearranging these modular units, TendrilBot can transform into a robotic arm with four or more degrees of freedom, significantly enhancing its manipulative capabilities. In addition, two types of locomotion are demonstrated. When connected in a linear configuration, TendrilBot exhibits locomotion through a sinusoidal motion pattern, similar to sidewinding. When connected in a circular configuration, TendrilBot can achieve locomotion via rolling with steering capabilities, utilizing its cylindrical or helical shape, respectively. Presented are detailed design configurations and characterization of TendrilBot functionalities and capabilities. In addition, we developed a data-driven model that can accurately capture bending of the modular soft actuators, which was validated by the experimental results. Comparison with other similar modular soft robots is provided and discussed. Extensive experimental validations are performed to showcase TendrilBot's potential for diverse applications in the field of modular soft robotics.

1. Introduction

The field of modular soft robots is an ever-growing field, with advancements in soft robotic actuators, tactile sensors, connectors, and materials. The development of soft robots has allowed for increased flexibility, adaptability, and versatility in various applications, especially those with close human interaction and pushed the boundaries of soft robots [1]. Creation of modular soft robots that can be assembled and reconfigured easily can enable rapid customization for specific tasks or environments. With their ability to deform, conform, and interact safely with humans and delicate surroundings, modular soft robots hold immense potential in fields such as healthcare, search and rescue, and exploration in challenging terrains [2]. Moreover, they boast capabilities such as modulating stiffness to adjust to different tasks or environments [3], locomotion for traversing diverse terrains [4], and grasping objects with dexterity [5], making them highly adaptable and functional across a wide range of scenarios. This growing technology promises to revolutionize industries by offering innovative solutions to complex problems while pushing the boundaries of what robots can achieve.

The elemental units of modular soft robots typically integrate soft actuators with rigid components for interunit connectivity, enabling reconfiguration and facilitating diverse functionalities [2]. One key advantage that is observed in many of these modular soft robots is their ability to modulate stiffness, often achieved through system pressurization [3,6]. This feature proves particularly useful in tasks such as object manipulation, where the flexibility of the robotic arm can be adjusted to suit different objects and tasks. Moreover, soft robot designs showcase a variety of motion capabilities, including rolling [4,5,7,8] crawling [7–11], and sinusoidal [8,12] movements. These motions are facilitated by the utilization of air pressure or vacuum, enabling both translational and rotational motion, thus enhancing adaptability in navigating diverse environments. Among the most desirable functionalities of modular soft robots is their adeptness at grasping objects. In

* Corresponding author.
E-mail address: trkov@rowan.edu (M. Trkov).

https://doi.org/10.1016/j.sna.2024.115835
Received 17 April 2024; Received in revised form 14 August 2024; Accepted 22 August 2024
Available online 23 August 2024

comparison to their rigid counterparts, soft robots excel in this area due to their ability to conform to the shape of the objects they grasp, thereby increasing effectiveness and versatility [3,13]. While these designs offer considerable value and efficiency in performing specific tasks, they often fall short of true versatility. Despite their capabilities, further advancements of these soft modular robots are needed to enable them to achieve a broader range of functionalities and adopting them for wide range of applications.

This paper introduces a soft, modular, and reconfigurable robot configuration designed to modulate its radial stiffness and grasping functionality, enhancing adaptability for versatile operational tasks (Fig. 1). Departing from conventional soft robotic systems [2,14,15], the proposed robot features a distinctive tunable interlocking mechanism utilizing permanent magnets with coils (PMC) for connectivity. This interlocking mechanism previously developed by our group [16] allows for adjustable inter-module connections at both tips and sides of the modules. The improved connectivity enables the assembly of elemental soft actuators in parallel or series configurations, facilitating planar or spatial system formations. Herein, we highlight the performance of the snake-like robotic configuration TendrilBot robot, where its linearly connected pneumatic actuators demonstrate capabilities of radial grasping, accommodating various shapes and sizes. Through experimental testing we validated the effectiveness of this robot in performing radial grasping tasks through insertion or wrapping (Fig. 1b-c), radial stiffness modulation (Fig. 1c), multi-degree of freedom soft manipulator assembly, and locomotion, showcasing its advanced functionalities and capabilities. In addition, a data-driven model of our modular soft actuator was developed that captures its mechanical performance as validated through experiments. The main contributions of this paper are threefold. First, we demonstrated the reconfiguration capabilities of identical modular actuators and showcased the resulting changes in structural morphology as well as the enabled modulation of radial stiffness, radial grasping, spatial actuation, and locomotion within a single robotic system. The characterization of each of these capabilities was carefully carried out and presented in detail. Second, we developed a data-driven model of the modular soft actuator and validated it through comparison to the experimental results. We present discussions on the advantages and limitations of these data-driven models in modular soft robots. Last, we analyzed the existing linear-type modular soft robots and quantified their performance against our actuator in terms of stiffness modulation, locomotion, manipulation, grasping abilities, and adaptability.

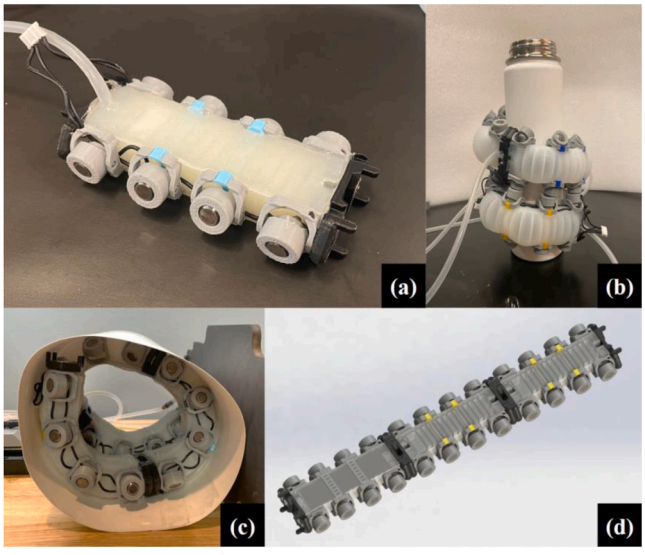

Fig. 1. Overview of a basic unit and representative TendrilBot configurations. a) A single modular unit used in all robot configurations. The actuator can bend in one direction and connect to other units at its tips or sides. b) TendrilBot wrapped around a metal water bottle. c) TendrilBot wrapped along the interior of a highly deformable paper cylinder for investigating radial stiffening. d) CAD view of a TendrilBot configuration, featuring three actuator units connected in series. The end connectors allow both bottom up (left unit) or bottom down (center and right units) actuator orientations to achieve bending in opposite directions.

In the following sections, we first briefly discuss the design features of the elemental actuators as they pertain to the assembly of TendrilBot. Then, we develop a data-driven model of an elemental unit in free-boundary displacement using Sparse Identification of Nonlinear Dynamical Systems (SINDy) [17]. We discuss the learned model within the scope of Tendrilbot, and the field of modular soft robots as a whole. Next, we show the grasping capabilities of the TendrilBot configuration and results of holding and squeezing force capacities. We then demonstrate the robot's proficiency in grasping hollow objects through insertion and expansion of the actuators. Following is a demonstration of TendrilBot's capacity to modulate radial stiffness by connecting the side PMCs. Subsequently, we present an alternative TendrilBot configuration that enhances the capabilities of these modular units through the assembly of a multi-degree soft robotic arm. We then present two methods of TendrilBot locomotion capabilities. Lastly, we discuss potential alternative uses for these modular actuators, examine their limitations, assess their potential impacts on the field of soft robotics, compare performance with other similar robots, and explore diverse applications for this innovative technology.

2. Modular pneumatic actuator

2.1. Modular pneumatic actuator design

The TendrilBot consists of several modular pneumatic actuators (MPAs) that have been previously developed and characterized in [16]. Herein, we briefly describe the design of MPA for completeness and primarily focus on describing the design features that enable serial assembly of MPAs to form TendrilBot and enable its functionality. The MPA is composed of several soft and hard components designed for actuation and seamless interconnection between units, respectively (see Fig. 2). At its core, the actuator features a Pneumatic Network (PneuNet) [18] crafted from silicone rubber material (Dragon Skin 10, Smooth-On, Macungie, PA) with Shore 10 A hardness. This network has integrated a fiberglass mesh at the actuator's base, serving as an inextensible layer crucial for enabling bending movements. Construction of the pneumatic network actuators involves a process using a two-part mold system: an upper mold responsible for creating the air chambers and upper body, and a lower mold housing the fiberglass mesh and lower hinge supports.

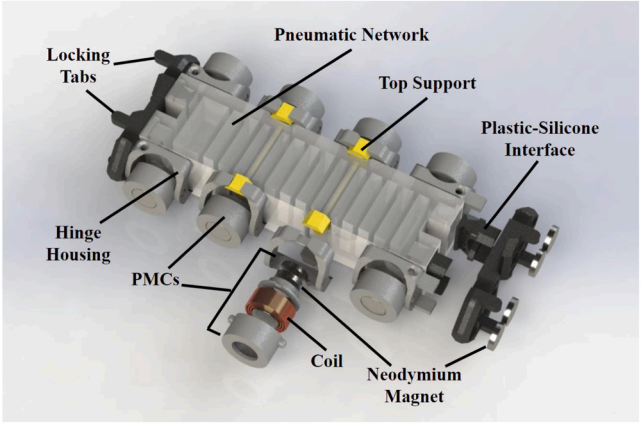

Fig. 2. Design of the Modular Pneumatic Actuator (MPA). Schematics show various hard and soft components of the elemental actuator, including the end and side connectors, permanent magnets with coils (PMCs), permanent neodymium magnets, and molded silicone pneumatic network actuator.

Upon completion, the two molds are securely joined with additional silicone rubber. Application of positive air pressure inflates the chambers within the PneuNet, causing their expansion and exerting force between them. The inherent softness of the actuator's top and bottom contact surfaces enables versatile grasping functionalities, both internally (through insertion) and externally (by wrapping around), by leveraging the inflation of chambers and the bending force of the actuators, respectively. All the components, including silicone rubber, fiberglass mesh, magnets, wires, and plastic 3D filament, are low cost and the actuators can be constructed using inexpensive fabrication methods, requiring only a FDM printer.

The versatile and carefully designed dimensions of the actuators facilitate various assembly configurations, offering adaptability to diverse robotic designs. Each unit measures 120 mm in length, 60 mm in width, and 25 mm in height, dimensions conveniently aligned in multiples of 30 mm. Height was intentionally designed to be slightly smaller than 30 mm to allow stacking them together (as shown in Section 3.4). This carefully selected design choice enables seamless assembly in multiple orientations, including end-to-end, end-to-side, and side-to-side arrangements. While the TendrilBot configuration primarily showcases two connection types—end-to-end for linear robot structures and side-to-side for radial configurations—the possibilities extend beyond these examples.

At each end of the modular actuators, a 3D printed end plate serves as a crucial component, incorporating permanent neodymium magnets and locking tabs. These magnets play a pivotal role in ensuring robust connections between modules, while the locking tabs prevent any shifting during the presence of shear loads and secure the hinges in place when utilized in TendrilBot configurations and beyond. Notably, unlike conventional modular soft actuators, these MPAs feature side magnets, expanding the array of possible connection methods and combinations. The magnets on the side of MPAs are strategically positioned within articulating hinges, firmly secured by top and bottom supports inserted through the silicone actuator. Housed within these magnet compartments are PMCs that enhance the versatility of the system. These PMCs facilitate controlled disconnection of the actuators without requiring manual intervention. By supplying power through the coils, the magnetic field of the permanent magnets can be temporarily neutralized, allowing for effortless disconnection of modules. Additionally, the direction of the current can be reversed to temporarily reinforce connections, especially in scenarios where the robotic system encounters elevated loads, such as during grasping objects.

We form circular and helical configurations of TendrilBot to demonstrate its grasping and squeezing capabilities. Similar configurations are used to showcase the internal grasping (through insertion and inflation) as well as modulation of radial stiffness of TendrilBot and surrounding flexible circular objects. Control of PMCs at the sides was utilized to tune the interunit connectivity and modulate radial stiffness of the TendrilBot/object structure and shows the effectiveness of such configurations in tasks such as object manipulation and reinforcement of hollow cylindrical objects. Alternative configuration of linearly connected actuators to form a multi-degree of freedom actuator is presented to demonstrate its expanded capabilities. Linear and cylindrical configurations are formed to demonstrate locomotion capabilities.

2.2. Data-driven modeling of modular pneumatic actuators

The series structures of PneuNets within the MPAs cultivates a complex kinematic and dynamic response that is a formidable modeling problem. While there exist work exploring the modeling of forms of PneuNets [19], the interplay between the sections between the supports in our MPAs leads to a nonuniform inflation profile that is better suited for data-driven modeling. There is a broad assortment of methods to construct dynamic models of systems from a set of observables such as empirical dynamic modeling, neural networks, Koopman operators, and SINDy [20]. In the long lists of possible methods for systems identification, black-box methods may be undesirable in some applications as they lack interpretability. The Koopman and SINDy methods are particularly powerful as they provide interpretable models which can be easily used with well-established controls methods. Relevant to soft robotics, Koopman has been used for dynamic modeling and model predictive control of a soft robotic arm [21,22], and SINDy has been used to construct a controller for end effector positioning in a soft robot [23] and for nonlinear model predictive control of a soft robotic esophagus [24].

Herein, we focus on identifying a model using SINDy with control [25]. SINDy is a method for dynamical system discovery that uses sparse regression. The method leverages the fact that many dynamical systems are governed by a few terms, that is, the governing equations are sparse in a function space, making it a tractable search. In our model using SINDy we considered our actuators as a dynamical system with state vector $\boldsymbol{x} \in \mathbb{R}^n$, and inputs $\boldsymbol{u} \in \mathbb{R}^q$ as shown in Eq. 1:

$$\frac{d}{dt}\boldsymbol{x} = f(\boldsymbol{x}, \boldsymbol{u}), \quad \boldsymbol{x}(0) = \boldsymbol{x}_0 \tag{1}$$

A time history of the state and control were arranged into matrices $\boldsymbol{X}$ and $\boldsymbol{U}$, and their time derivatives were numerically approximated. A library of nonlinear candidate functions $\boldsymbol{\Theta}(\boldsymbol{x}, \boldsymbol{u})$ was constructed, which in our work consisted of polynomial functions up to the third order and has cross coupling between the states and control. A sparse regression problem was set up to find a vector of coefficients $\boldsymbol{\Xi} = [\xi_1 \quad \xi_2 \quad \ldots \xi_n]$ to determine which elements were significant as shown in Eq. 2:

$$\dot{\mathrm{X}} = \boldsymbol{\Xi}\boldsymbol{\Theta}^{\boldsymbol{T}}(\boldsymbol{X}, \boldsymbol{U}) \tag{2}$$

For the k-*th* row of $\boldsymbol{\Xi}$ we determined the coefficients by solving the sparse regression problem in Eq. 3, where λ is a sparsity promoting hyperparameter:

$$\boldsymbol{\xi}_k = argmin \frac{1}{2}||\dot{\mathrm{X}}_k - \widehat{\boldsymbol{\xi}}_k \boldsymbol{\theta}^{\boldsymbol{T}}(\boldsymbol{X}, \boldsymbol{U})||_2^2 + \lambda||\widehat{\boldsymbol{\xi}}_k||_1 \tag{3}$$

We collected a pressure-displacement history of an MPA where states x_t and y_t describe the tip motion of the actuator relative to a fixed base at point (x_0, y_0), and the control input P, to perform system identification using SINDy [26,27]. We considered the pressure as a control input due to the time-dependent mechanical response of the elastomeric materials. The pressure-time profile is shown Fig. 3a, where we have also added an annotated photograph of the actuator marking the base point, and tip as an inset. Displacement data are shown in Fig. 3b. Photographs of the actuators are shown as insets in various regions of motion. At first the actuator axially and radially expands as shown in (i) at 16.5 kPa. The actuator then continues to bend with the tips motion saturating around step 90. The inset (ii) was taken at 46.1 kPa. Last, the actuator curls in around 58.3 kPa as shown in (iii).

We present two SINDy models along with the displacement history in Fig. 3c. One model has linear library elements, which when formulated in discrete time is equivalent to DMD with control [28]. The second model in Fig. 3c is a higher order fit which better captures the system's dynamics. The L1 error is presented in panel (d). We anticipated that lower order models may have a hard time capturing the multi regime state response, even if the dynamics are smooth. As such we investigated multiple models. We were particularly interested in an equivalent DMD model, due to DMD's relationship to Koopman methods. We find both models had a more difficult time characterizing the horizontal motions of the actuator, with the peak error in the 1st order model being 9.35 mm and the peak in the 3rd-order model being 3.35 mm. Excluding the end of the time history the error for the 3rd order model is

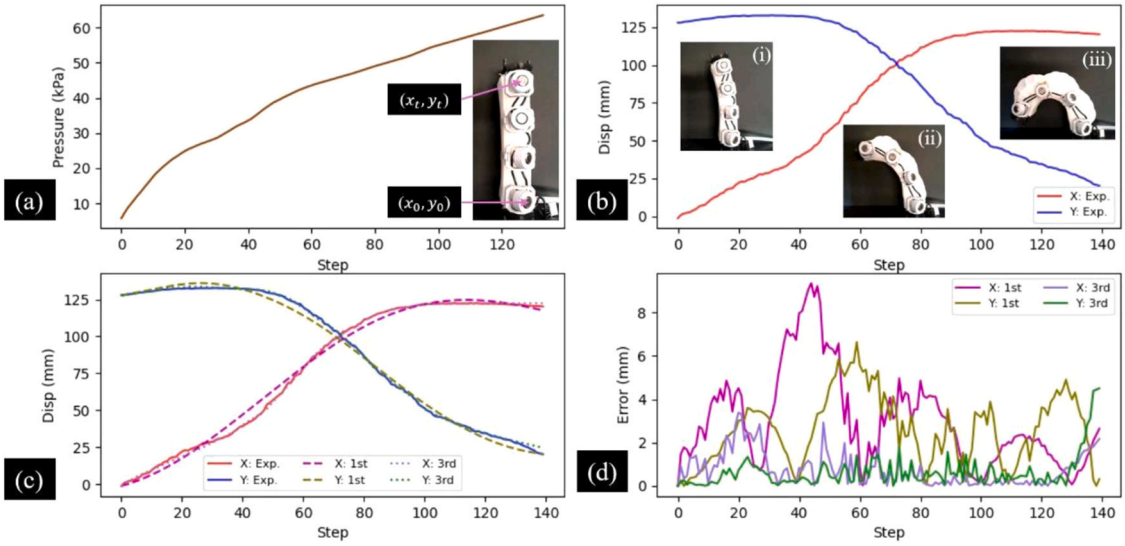

Fig. 3. MPA data-driven modeling. a) Pressure-time profile with an annotated photograph of an MPA showing data extraction points. b) Displacement data of the representative actuator with key points in pressurization shown as insets. c) Comparison of SINDy models with experimental data. The first order model corresponds to legend items with the designation 1st, and the 3rd order model corresponds to items with the designation 3rd. d) L1 error of SINDy models relative to the experimental data.

considerably lower than the first order model. Interestingly, both models performed well in the presence of the saturation behaviors highlighted in panel (b). It remains a topic of future work to investigate hybrid models for possible improved performance. The results signal that the flexibility of SINDy can lead to a significantly better model for soft robotic control with an appropriate selection of candidate functions.

To better understand the dynamics, we provide the identified 3rd-model in Eqs. (4), (5) for x_t and y_t, respectively.

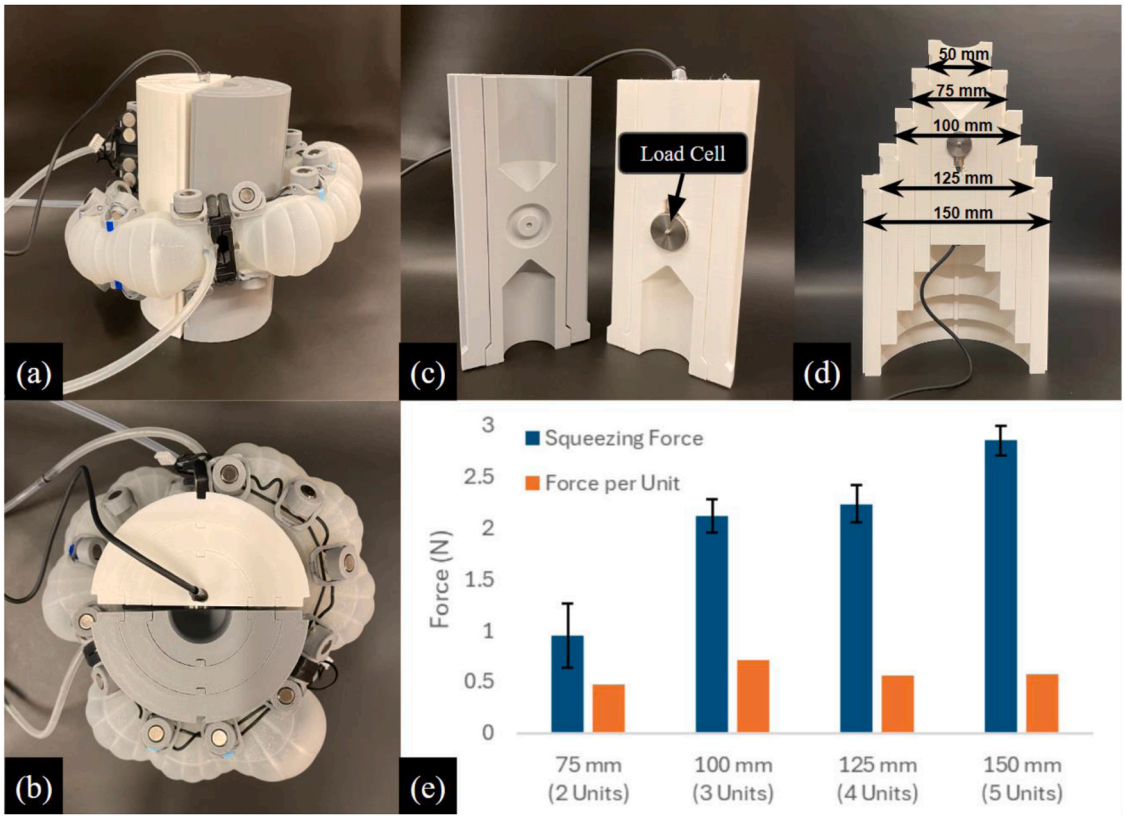

Fig. 4. TendrilBot's squeezing experiments. a) TendrilBot three-unit configuration wrapped around a 3D printed squeezing test apparatus with diameter of 100 mm. b) Top view of squeezing test showing the gap in between the two halves of the cylinders. c) Testing setup showing the load cell embedded in one side of the 50 mm diameter cylinder. d) Stacked 3D printed sleeves used to increase the squeeze testing diameter from 50 mm to 150 mm in 25 mm increments. e) Results of the squeezing force at different cylinder diameters and number of units. Force per unit is also presented as a standardization of the data, identifying the optimal grasping diameter. Applied air pressure in all tests was 8 psi (55 kPa).

$$
\begin{aligned}
x_t[\mathrm{k}+1] \;=\; & 29.691 \;+\; 0.725\; x_t\;[\mathrm{k}] \;+\; 0.182\; y_t\;[\mathrm{k}] \\
& -\; 0.405\; P\;[\mathrm{k}] \;-\; 0.003\; x_t\;[\mathrm{k}]^2 \\
& +\; 0.008\; x_t\;[\mathrm{k}]\; P\;[\mathrm{k}] \;-\; 0.003\; y_t\;[\mathrm{k}]^2 \\
& +\; 0.005\; y_t\;[\mathrm{k}]\; P\;[\mathrm{k}] \;-\; 0.001\; P\;[\mathrm{k}]^2
\end{aligned} \tag{4}
$$

$$
\begin{aligned}
y_t\;[\mathrm{k}+1] \;=\; & 204.520 \;-\; 5.980\; x_t\;[\mathrm{k}] \;-\; 0.584\; y_t\;[\mathrm{k}] \\
& +\; 3.592\; P\;[\mathrm{k}] \;+\; 0.078\; x_t\;[\mathrm{k}]^2 \\
& +\; 0.058\; x_t\;[\mathrm{k}]\; y_t\;[\mathrm{k}] \;-\; 0.055\; x_t\;[\mathrm{k}]\; P\;[\mathrm{k}] \\
& -\; 0.036\; y_t\;[\mathrm{k}]\; P\;[\mathrm{k}] \;-\; 0.108\; P\;[\mathrm{k}]^2 \\
& -\; 0.002\; x_t\;[\mathrm{k}]^2\; P\;[\mathrm{k}] \\
& -\; 0.001\; x_t\;[\mathrm{k}]\; y_t\;[\mathrm{k}]\; P\;[\mathrm{k}] \\
& +\; 0.004\; x_t\;[\mathrm{k}]\; P\;[\mathrm{k}]^2 \\
& +\; 0.002\; y_t\;[\mathrm{k}]\; P\;[\mathrm{k}]^2 \;-\; 0.002\; P\;[\mathrm{k}]^3
\end{aligned} \tag{5}
$$

A small threshold of 0.001 was used when finding the SINDy model, as such there are many terms which do not contribute much to the dynamics (i.e., on the order of 10^{-3}). However, we do observe in Eq. 5 that there is non-negligible cross coupling and at least a non-negligible quadratic in the horizontal motion and the control. In future iterations of these modules and applications using PneuNets such as Tendrilbot, these results may help inform the design and development of low-level controllers.

3. Experimental results

3.1. Grasping capabilities

The TendrilBot configuration exhibits versatile grasping by wrapping around objects of various sizes (Fig. 4). To assess its squeezing strength (radial force) during grasping, a setup similar to the one in [29] was devised to measure the exerted force. The setup involved placing a force sensor (LTW-08, DRMEE, China) between two 3D printed half-cylinders to measure the applied force (Fig. 4c). The diameter of cylindrical objects varied from 50 to 150 mm (Fig. 4d), where the smallest cylinder (50 mm) was only used to hold the sensor.

The number of actuators used for testing increased with each diameter, allowing for one complete revolution around the cylinder. In all wrapping tests, the applied air pressure was 8 psi (55 kPa). By limiting the pressure to this value, we prevent overinflation, permanent deformation, or damage of the actuators from repeated actuations. Results presented in Fig. 4e show a general increase in total squeezing force with the increase of diameter and the number of MPA units and reveal that 100 mm is an optimal diameter for achieving the highest force-to-unit ratio. Notably, the 100 mm cylinder diameter demonstrated the best match with the actuators' aperture, resulting in the highest squeezing force per unit (0.7 N). This diameter coincides with the functional length of the actuator (when subtracting the rigid connectors and their end attachments), which allows the actuator to bend with a smallest curvature and evenly distribute exerted force compared to other configurations and thus provides an optimal grip of an object. Subsequent tests were conducted using this optimal diameter to measure

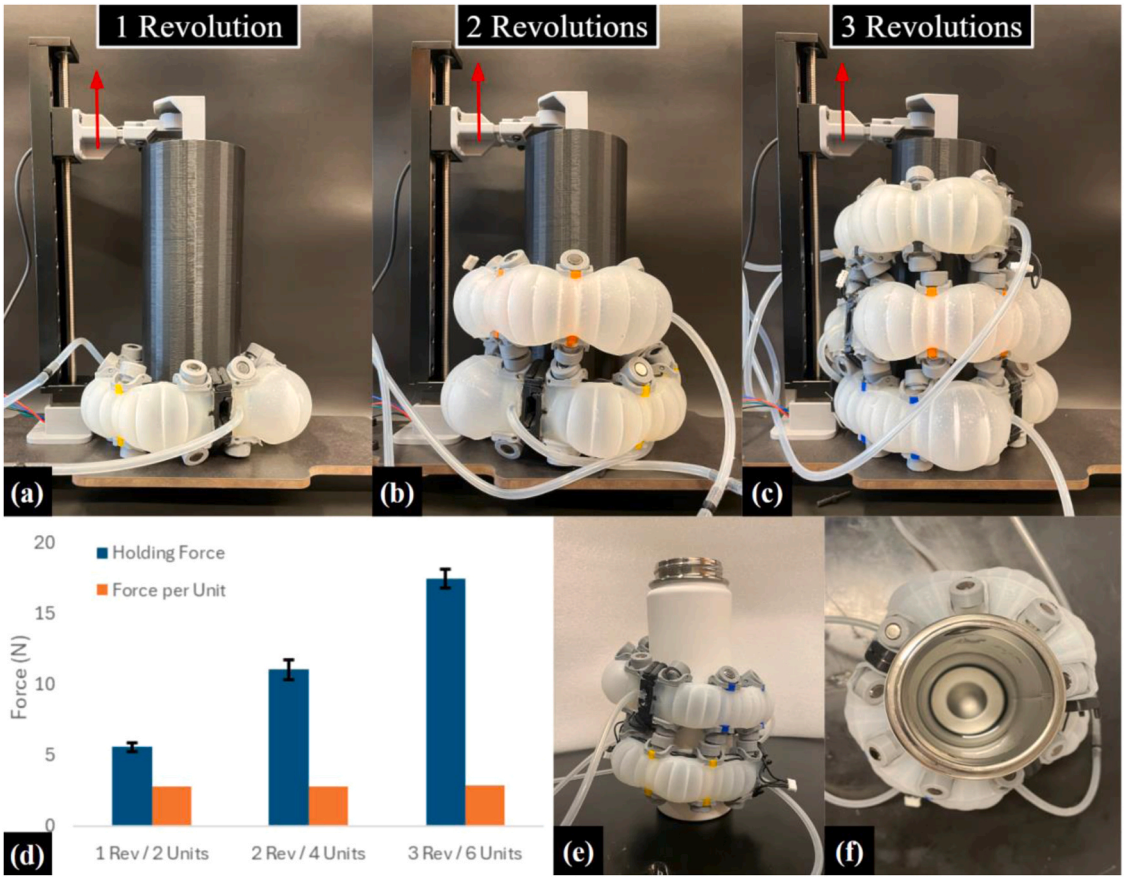

Fig. 5. Grasping capabilities. Experimental setup for measuring TendrilBot's holding force for a) one, b) two, and c) three revolutions around a 3D printed cylinder. In all tests, the cylinder was pulled upward by a linear stage, and the maximum force reached was measured by a load cell and recorded. Each actuator was pressurized to 8 psi in all tests. d) Results of holding force test. Normalized results shown in orange color show the holding force per unit used in TendrilBot. e) Side view and f) top view of TendrilBot (4-unit configuration) wrapped around a metal water bottle, which is 80 mm in diameter, to show that the TendrilBot can grasp metal objects without affecting the PMCs.

the holding (axial) force.

Investigating the holding capacity of maximum axial force that the TendrilBot can withstand when wrapped around the cylindrical object of 100 mm in diameter was performed as shown in Fig. 5. Various configurations of TendrilBot, consisting of 2, 4, and 6 units, were wrapped around a cylinder, achieving one, two, and three revolutions, respectively (Fig. 5a-c). To secure TendrilBot during testing, the side PMCs were utilized, anchoring it to a metal plate resting on the ground, while the cylinder was lifted vertically using a linear actuator (see Supplementary Movie S1). A load cell attached to the linear actuator captured the maximum force applied before an object experienced slippage, while PMCs remained connected to the steel plate. Fig. 5d shows the results of a direct correlation between the number of units employed and TendrilBot's maximum holding force. Across all revolution counts (one, two, and three), the average maximum force recorded was 5.6 N, 11 N, and 17.5 N, respectively. A consistent linear increase in holding force is observed with the increased number of revolutions. Notably, the holding force per unit remained consistent across all tests, averaging 2.8 N per unit for all configurations. These findings provide valuable insights for users seeking to determine the required number of modular units for specific grasping tasks with desired payload. It is important to note that while a pressure of 8 psi was maintained for all actuators, variations in the frictional properties of the grasped object and contact area size may affect these values. Nonetheless, this experimentation validates

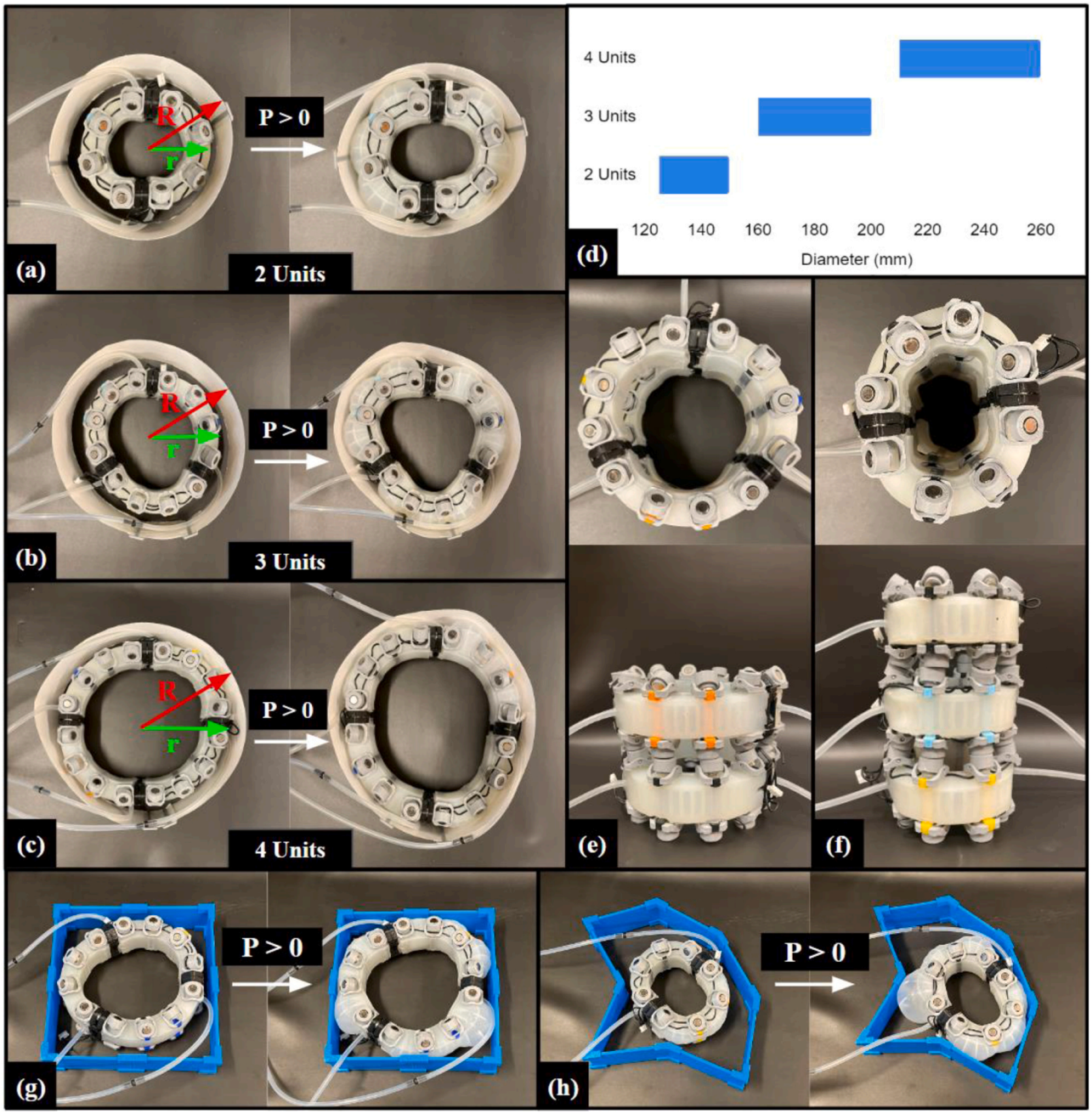

Fig. 6. Radial grasping configurations. TendrilBot in closed-form configurations with a) two (r = 120 mm, R = 150 mm, b) three (r = 160 mm, R = 200 mm), and c) four (r = 210 mm, R = 260 mm) modular units, where r is the outer radius of TendrilBot before inflation and R is the inner radius of the grasped cylinder. d) Range of cylindrical object diameters that can be grasped by TendrilBot with various numbers of units. Stacked closed-form TendrilBot units in e) two and f) three-layer configurations consisting of two units per layer. TendrilBot in a closed-loop state grasping g) square and h) irregularly shaped objects shown before and after inflation of actuators. The inflations of the chambers fill up the empty space between the actuators and the walls of the object to secure the grip on the handled object.

TendrilBot's holding capabilities.

One concern with the units, especially in their TendrilBot configuration, was how the PMCs would behave when the robot grasps metal objects. This is because the PMCs could become disengaged in the presence of a magnetically sensitive metallic object or surface. Figs. 5e and 5f show the experimental test of the TendrilBot grasping a metal water bottle, demonstrating that the functionality was fully preserved. The PMCs had higher attraction forces to one another than to the metallic object they were grasping. The reason is that the primary orientation of the PMCs is normal to the side of the actuators, which in turn favors the interconnectivity between the neighboring PMCs as their magnetic fields are aligned. This finding indicates that the TendrilBot can be used in a greater number of industrial applications, especially when they are used for grasping or manipulating metallic objects.

3.2. Inner-radial grasping capabilities

The TendrilBot system does not only grasp by wrapping around but can also facilitate radial grasping of a variety of sizes and shapes of hollow objects by insertion. The unique modularity feature enables the serial assembly of variable numbers of MPA units based on the shape and size of the hollow openings on the grasped objects. For example, in the simplest case such as a cylindrical opening in the body of an object, the number of the modular units can be easily configured to adapt to different radial dimensions of those openings. This adaptability proves particularly advantageous in scenarios where a single robotic system needs to handle a spectrum of tasks involving grasping objects of varying sizes.

Fig. 6a-c show the TendrilBot's ability to easily assemble different numbers of modular units that can pick up cylinders with diameters ranging from 120 mm to 260 mm by adjusting the number of units involved in the assembly. Fig. 6d shows the range of diameters that can be grasped for configurations consisting of 2–4 units. The results from experimental testing show that there exist diameters that the units are not capable of picking up. This gap could potentially be closed by using different chamber designs in the pneumatic network or higher pressures, which would allow the actuators to expand even further and increase the diameters that can be grasped; however, such testing was out of the scope of this paper. The max pressure used in this study was 8 psi to prevent permanent deformation to the actuator. Overall, the demonstrated dynamic configurability of the TendrilBot not only showcases the versatility of the proposed robotic system but also enhances its applicability across a wide range of industrial, manufacturing, and logistical scenarios.

In addition to its capabilities in grasping, the modular units play a pivotal role in increasing the radial stiffness of objects when TendrilBot is inserted inside, particularly cylindrical structures such as pipes. By strategically configuring and activating the modular units, the robotic system can effectively enhance the structural rigidity of an object, such as a pipe, enhancing its radial strength. This can be useful for repairing damaged pipes by temporarily enhancing the pipe's radial strength from inside and removing the actuator after repair is complete. These closed-looped configurations of TendrilBot can be stacked on top of one another (Fig. 6e-f), allowing for increased grasping and radial stiffness capabilities by increasing area of support along the object. This feature extends the utility of the system beyond traditional grasping tasks, showcasing its multifunctionality in tasks requiring structural support or stabilization. Experimental validation of modulating radial stiffness is presented in Section 3.3.

The ability of TendrilBot to grasp objects extends beyond cylindrical shapes to encompass a wide array of forms. Due to the inherent softness of the actuators, they can conform to the contours of various objects,

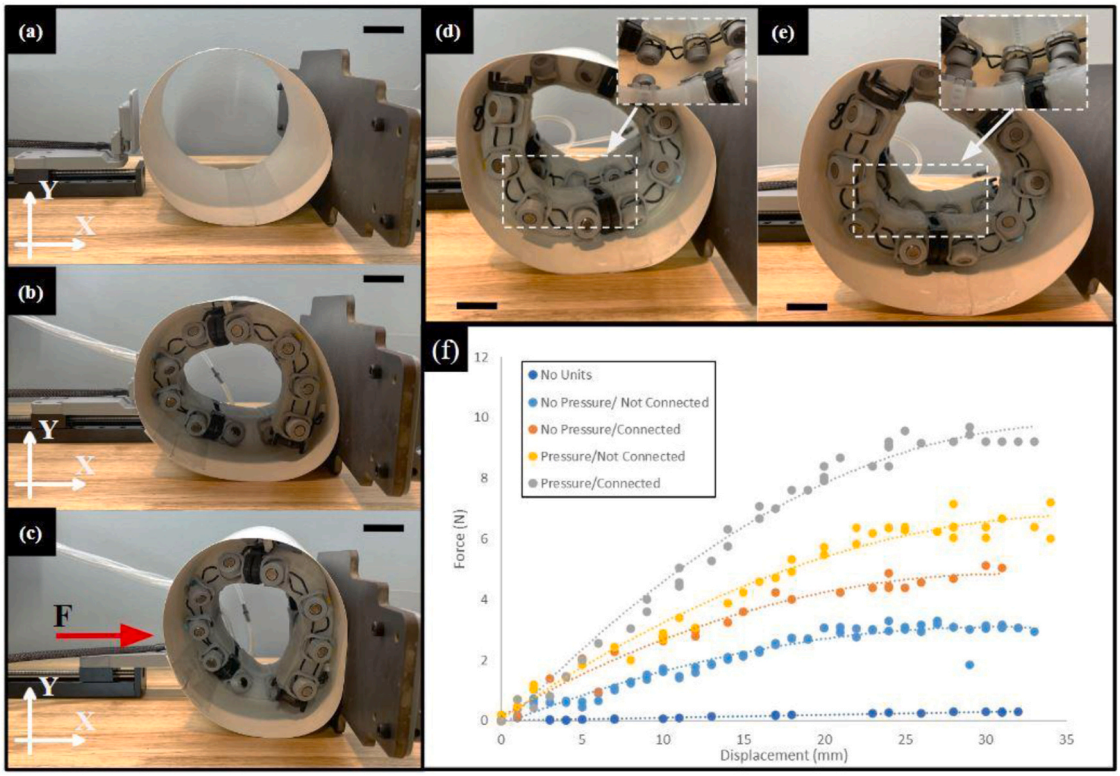

Fig. 7. TendrilBot increases radial stiffness of a tubular object. a) Experimental setup for radial stiffness test showing a compliant paper cylinder and a force sensor fixture on a linear actuator that pushes radially against the cylinder from outward. b) TendrilBot inserted inside a paper cylinder and inflated. c) Deformed cylinder after being radially pressed by a force sensor fixture. TendrilBot with pressurized units in d) disconnected and e) connected PMC states. f) Radial stiffness of TendrilBot in different configurations with units in pressurized and unpressurized states, with connected and disconnected PMCs. Results show data from three tests for each configuration with overlaid best fit curve. Scale bar: 30 mm.

including those with rectangular or irregular shapes. Fig. 6g-h illustrate closed-loop TendrilBot configurations comprising two or three units, demonstrating their capability to securely grip non-cylindrical objects in a closed-loop state. This versatility stands as a significant advantage of soft robots over their rigid counterparts in grasping tasks, as they can accommodate a broader range of objects, offering enhanced adaptability and functionality.

3.3. Modulating radial stiffness

An important advantage of TendrilBot is its ability to linearly connect MPA units and insert it within the interior of a circular object (e.g., pipe/tube) in a spiral shape to increase the structure's radial strength. The TendrilBot can be pushed and fed inside along the object to reach a specific location and lock in a desired shape or diameter size by engaging side magnets, where upon simultaneous pressurization of MPA units, the TendrilBot provides radial support. This actuation effectively strengthens the structure and increases its radial stiffness.

We performed multiple tests to demonstrate the effectiveness of using the TendrilBot to modulate its own stiffness and maximize the overall stiffness of a tubular structure. Fig. 7 shows the testing setup that consisted of a compliant, paper cylinder with a diameter of 150 mm and the TendrilBot, in its wrapped-around form, which was inserted to fit the interior of the cylinder. As the number of turns of the TendrilBot plays a role in the measured stiffness, we kept this variable at a constant of 1.5 turns in our experiments and utilized the same four units in all radial stiffness tests. The force sensor fixture mounted on a linear actuator was pushed against the outer surface of a compliant cylinder to measure the applied force and a linear actuator was used to simultaneously measure the radial displacement (Fig. 7a-c and Supplementary Movie S2).

The unique ability of the TendrilBot is when the soft actuator units are linked together sideways by engaging the side PMCs. This engagement allows the robot to maintain its radial shape even when the MPA units are not pneumatically actuated by locking the actuators in place and therefore increasing its radial stiffness or strength. Fig. 7 shows results of various configurations with or without applied pressure and with or without connected PMCs. A setup with inserted TendrilBot and connected PMCs but with no air pressure showed an increased stiffness of the paper cylinder by 4 times of its original value. When the units were pressurized but with the PMCs disconnected (Fig. 7d), the stiffness increased an additional 50 %, from about 4 N to 6 N at a displacement of 30 mm. The engagement of the side PMCs along with pressurization, as shown in Fig. 7e, resulted in the highest radial stiffness value, with a measured 10 N of force at 30 mm of displacement (Fig. 7f). The results of this testing show the TendrilBot's ability to significantly increase the radial stiffness of the object for more than an order of magnitude when inserted inside with the PMCs engaged and the actuation units pressurized.

3.4. Multi-degree of freedom actuation

The versatility of the modular pneumatic actuators enables connecting the MPA in advanced configurations, allowing creation of a soft robotic arm with multiple degrees of freedom. Fig. 8 shows an example of such an assembled soft robotic arm. In this specific configuration, two units are strategically positioned parallel to each other back-to-back (facing in the opposite directions), with the bottoms of these units serving as the bending axis for this actuation pair. To enhance the structure, a 3D printed adapter plate is affixed to the top of these two units, and another two units are added on top, while rotated 90 degrees from the initial pair. This arrangement forms a soft robotic arm with a 4 degrees-of-freedom capability (Fig. 8).

Experiments were performed to characterize the workspace of this soft robotic arm configuration. When the lower units were actuated with a pressure of 8 psi, the end effector of the robotic arm demonstrated a maximum bending angle of 75 deg from the vertical, reaching 150 mm horizontally from the center and 90 mm from the attached surface. Conversely, actuating only the top units allowed the robotic arm to achieve a bending angle of 80 deg and maximum reach of 110 mm from the center and 150 mm from the attached surface. By combining the

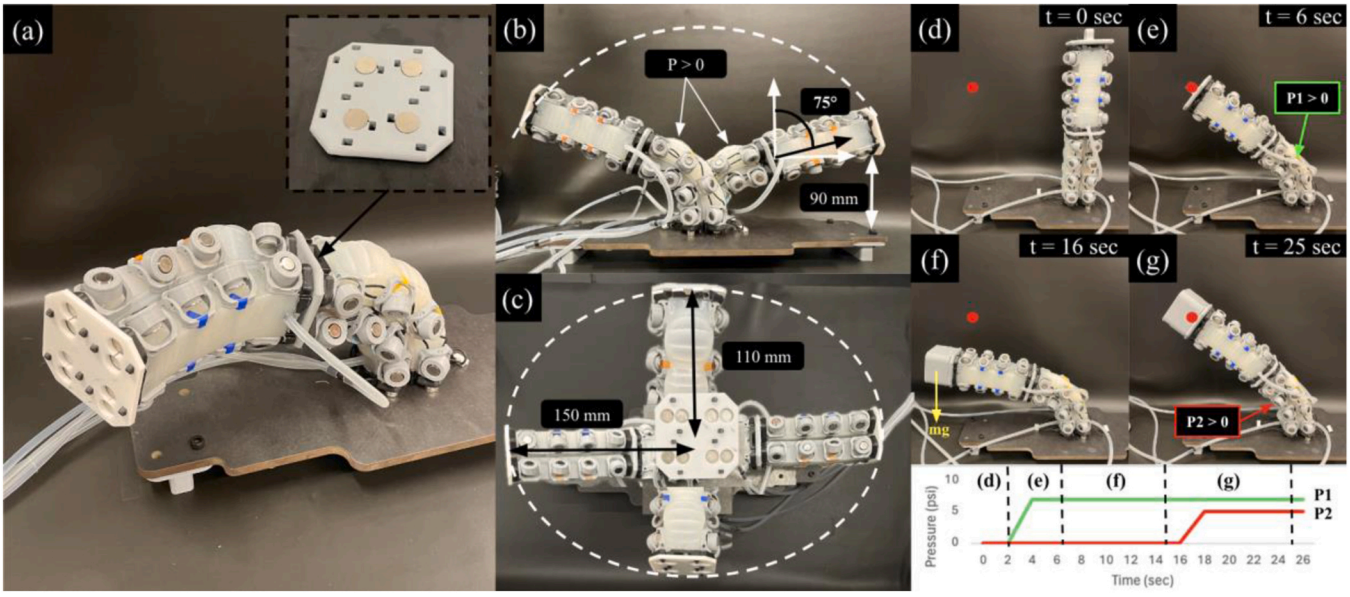

Fig. 8. Multi-degree of freedom actuator assembled from modular MPA units. a) Robotic arm constructed of four MPAs. Embedded image shows 3D printed plate used for alternating actuator direction when assembling linearly. Actuators are stacked back-to-back to allow bending in both directions. b) Bottom actuators are pressurized, with the end effector achieving a bending angle of 75 degrees from the vertical reaching 90 mm from the surface. c) Top-down view demonstrating the workspace that the robotic arm can reach on all sides from its base. (d-g) Load carrying and stiffening capabilities for various actuation states of actuators in the bottom module. The schematic under the figures demonstrates the pressure profiles that are color coded for each respective actuator (bottom left – red and bottom right – green) to show actuation sequence. d) Robotic arm unpressurized in a vertical position. e) One actuator of the bottom module is actuated/pressurized, bringing the end of the robotic arm to a desired point (marked as red dot). f) A mass (80 g) is added to end of the soft arm, causing it to deviate from the desired point. g) Opposing actuator in the bottom module is actuated, stiffening the robotic arm, and returning the end effector to its original position.

movements of all four units, the robot showcased its ability to navigate within the workspace shown in Fig. 8c through the manipulation of actuation profiles in all four chambers. The elliptical shape of the workspace is governed by the order of stacking of actuator pairs, where the major and minor axes are aligned with the bending direction of the bottom and upper actuator pairs, respectively. Furthermore, the robot exhibited the capacity to modulate its stiffness effectively by actuating opposing units, adding an additional layer of adaptability to its functionality. This stiffening capability allows these actuators to combat the gravitational and operational loads imposed on the soft robotic system, adding a higher degree of precision to the system (Fig. 8d-g). While control of the arm was out of the scope of this paper, an algorithm could be utilized in the future to automatically detect and correct deviation by regulating the pressure within the actuators. Overall, these results underscore the promising capabilities of these modular pneumatic actuators in enabling sophisticated and flexible robotic movements.

3.5. Locomotion

In addition to its grasping and radial stiffness capabilities, TendrilBot also exhibits versatile locomotion capabilities. Fig. 9a showcases a closed-chain TendrilBot configuration comprising three sets of two-unit closed chains stacked side-by-side. Notably, the units within each loop exhibit a 90-degree rotational offset from one another, enabling alternating inflation to generate rotational motion. This configuration demonstrates TendrilBot's ability to achieve locomotion through rolling (Fig. 9a). Control input schematics are presented at the bottom of Fig. 9a showing sequential pressurization/deflation of center and side units. This form of locomotion was able to achieve an average speed of 4.6 cm/s along the surface of a flat table. The steering is possible by respective inflation of the opposite side of the actuator closed chains with respect to the steering direction; however, the detailed control was out of the scope of this paper.

Alternatively, a linear version of TendrilBot displays a sinusoidal motion pattern producing a sideway locomotion (Fig. 9b and Supplementary Movie S3). By connecting four modular units linearly, with alternating bending directions, TendrilBot can execute sideways movement reminiscent of the sidewinding motion observed in nature, particularly in snakes [30−32]. This sideway motion averaged a speed of 0.31 cm/s, which could potentially be improved through gait optimization. This dual capability highlights TendrilBot's adaptability in various locomotion scenarios, showcasing its potential for diverse applications beyond simple grasping tasks.

4. Discussion and conclusion

Soft robots like TendrilBot offer distinct advantages over rigid robots, particularly in scenarios requiring close interaction with humans. The inherent compliance and flexibility of soft robots, such as the constructed multi-degree of freedom soft robotic arm (Fig. 8), make them safer to work in proximity to humans, minimizing the risk of injury or damage in collaborative settings [33,34]. Additionally, the ability of TendrilBot to conform to complex shapes and environments, as demonstrated through grasping of a complex shape object in Fig. 6,

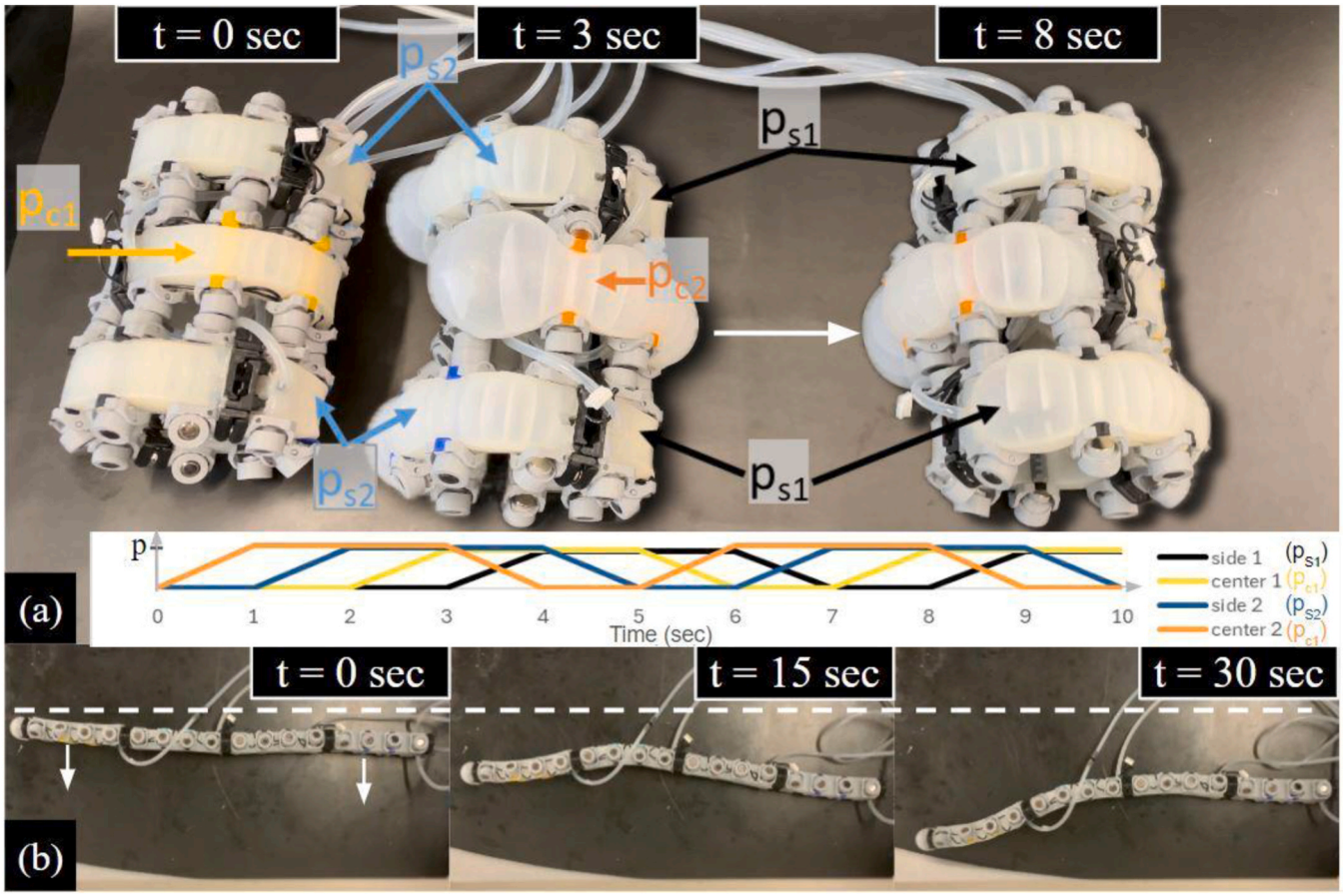

Fig. 9. TendrilBot locomotion capabilities. Two methods of locomotion can be achieved with various assembly of the modular units. a) The first consists of TendrilBot consisting of three stacks of two-unit closed-chains of MPAs radially offset for 90 deg forming a cylindrical shape. Through strategic inflation of the actuators (alternating side or center), a rolling motion can be produced, moving the robot forward or backward. The schematic under the figure shows the actuation sequence used to produce this motion. b) The second is a sinusoidal sideway motion, in which a TendrilBot configuration is placed on its side with alternating orientation of MPAs. Through actuation of the units in an alternating pattern, it moves sideways.

enhances their versatility and adaptability, enabling them to perform tasks that may be challenging or unsafe for its rigid counterparts. TendrilBot's modular nature also allows for rapid reconfiguration, facilitating quick adaptation to various tasks and environments. Its ability to grasp objects of different shapes and sizes, coupled with the capability to adjust stiffness on-demand, enhances its utility across a wide range of applications. Its innovative design and modularity allow for scalability, meaning the concept of modular soft robots can be adapted to different sizes, from centimeters to the meter scale [35,36]. This offers potential for the TendrilBot to be designed for various applications in industrial automation, agriculture, or healthcare. Moreover, the cost-effectiveness of TendrilBot is noteworthy, as a single low-cost modular unit costs only $20 to manufacture and does not require any specialized equipment other than a 3D printer. This inexpensive design can be used for multiple tasks, reducing the need for specialized equipment and lowering the overall implementation costs. Lastly, its modular nature allows it to be used in the educational setting similar to LEGO™ building blocks, where students can use their creativity and explore various robots' configurations to build functional structures.

Research in modular soft robots has led to the development of various designs, each showcasing different capabilities. Here we compare TendrilBot to three other linear-type soft modular robots in terms of stiffness modulation, locomotion, manipulation, adaptability, and grasping abilities (Fig. 10). The grading scale for each criterion was graded out of 10, with a higher score indicating better performance. These scores were determined by evaluating multiple calculated and analyzed parameters relative to the robots under comparison. Stiffness modulation was evaluated based on the robots' range of modulation and stiffness relative to their size (N/mm per cm^3). The size of the robots is an estimation of the volume (cm^3) based on dimensions provided in the articles. Similarly, locomotion capabilities were graded based on the robots' combined score of speed relative to size (velocity/cm^3) and its multimodal capabilities, which could include rolling, sidewinding, etc. Manipulation abilities were assessed by considering factors such as spatial ability (degrees-of-freedom and movement) and the precision and repeatability of actuator control. Grasping capabilities were evaluated by considering the holding strength (N/cm^3) and versatility in handling objects of different sizes and shapes. Adaptability was assessed by considering both the number of functions a single design could perform and its ability to adapt and be reconfigured to new situations, where quicker and simpler reconfigurability granted the design a higher score. This grading system enabled a comprehensive comparison of the robots' functionalities, enabling insights into their relative strengths and weaknesses.

Among existing linear-type modular soft robots, the design by Stella et al. [6] stands out for its exceptional stiffness modulation, capable of dynamically increasing stiffness by 300 % and achieving the highest N/mm per cm^3 (stiffness relative to size) among the compared soft robots. The vacuum-powered soft actuators developed by Robertson et al. [11] demonstrates impressive speed and multimodal locomotion capabilities, including rolling, inching, and even climbing. The calculated speed-to-size factor of 1.68, compared to the 0.9 for TendrilBot, along with the broad range of multimodal motion, earned this robot design the highest score in the locomotion category. However, both designs lack the versatility needed for diverse tasks. On the other hand, Karimi et al. [3] designed a robot that displays considerable versatility due to its ability to change morphology for navigation, excellent stiffness modulation (600 % stiffness increase), and strong grasping capabilities. Yet, it still falls short of the versatility demonstrated by TendrilBot. Overall, when comparing TendrilBot to these other linear-type soft modular robots, it emerges as a more versatile option, capable of a wider range of functions (Fig. 10). TendrilBot's unique interunit connectivity enables swift and effortless reconfiguration, facilitating tasks spanning from multimodal object grasping to locomotion. This adaptability sets TendrilBot apart as a highly versatile solution in the realm of modular soft robotics.

The limitation of the current TendrilBot design includes variations in chamber size between the center and distal or proximal chambers as well as imperfect fabrication of actuators. These led to uneven chamber deformations as can be observed in Fig. 6g-h. Improving the fabrication process by carefully inspecting the top wall thickness and creating even sized chambers in the future can improve the TendrilBot performance. One area of potential advancement for TendrilBot lies in the integration of sensors and implementation of control algorithms. By incorporating sensors (e.g., tactile, force, or bending) into the module units, TendrilBot could achieve autonomous manipulation and interaction with its surroundings, enhancing precision and control. These sensors could provide valuable feedback, enabling TendrilBot to adjust its grasping force or stiffness dynamically based on the task at hand. This would further expand TendrilBot's capabilities and increase its suitability for a wider range of applications. Our data-driven approach to understanding the robot dynamics serves as a first step in these endeavors.

In summary, this paper contributes to the field of soft robotics through the introduction of TendrilBot—a modular, reconfigurable robot configuration with versatile grasping, radial stiffness modulation, and locomotion capabilities. The TendrilBot can perform radial grasping

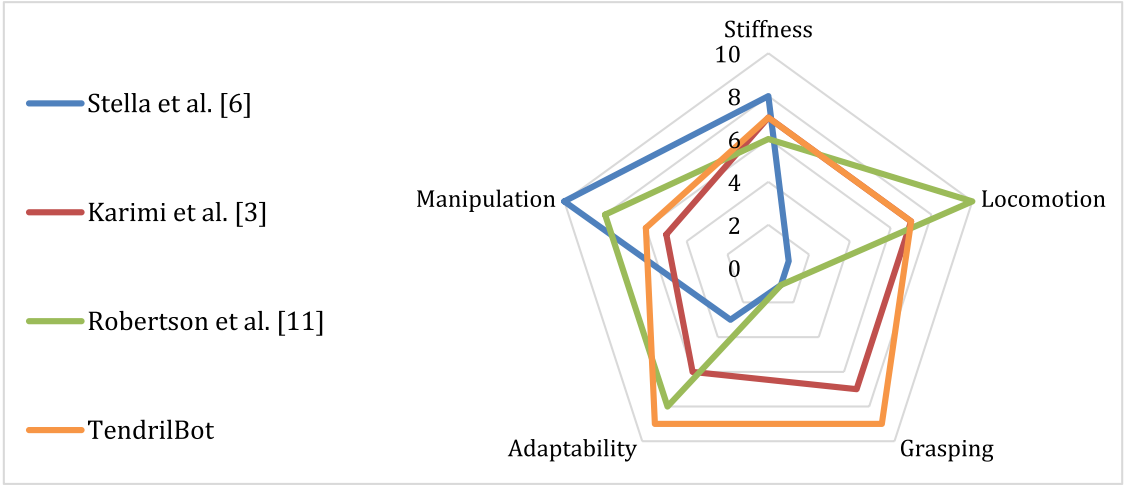

Fig. 10. Comparison of similar, linear-type modular soft robots. Among all five evaluated metrics, the TendrilBot performs well in all of them and outperforms other robots in adaptability and grasping. Representing the largest envelope in the presented plot signifies the TendrilBot's versatile capabilities, making it a preferred candidate as a single system capable of performing a large range of tasks.

tasks through insertion or wrapping. The innovative design of TendrilBot, featuring a unique interunit connection and the ability to adjust radial and linear stiffness, represents a significant advancement in soft robotic systems. In addition, the assembly of a multi-degree of freedom soft manipulator from modular actuator units further demonstrates the versatility of the developed system and expands its potential applications.

The future directions of TendrilBot involve enabling untethered capabilities and dedicated sensing and control to expand its uses further. This transition would enable TendrilBot to operate autonomously in various environments, opening new possibilities for potential applications such as search and rescue missions and terrestrial exploration.

CRediT authorship contribution statement

Mitja Trkov: Writing – review & editing, Supervision, Resources, Project administration, Methodology, Funding acquisition, Conceptualization. **Wei Xue:** Writing – review & editing, Supervision, Resources, Funding acquisition, Methodology. **Nicholas Paliocca:** Formal analysis, Methodology, Software, Validation, Visualization, Writing – review & editing. **Joshua Knospler:** Writing – original draft, Visualization, Validation, Methodology, Investigation, Formal analysis, Data curation, Conceptualization, Software, Writing – review & editing.

Declaration of Competing Interest

The authors declare that they have no known competing financial interests or personal relationships that could have appeared to influence the work reported in this paper.

Data availability

Data will be made available on request.

Acknowledgments

This material is based upon work supported by the National Science Foundation under Grant No. 2235647.

Author contributions

MT: conceptualized and designed the study and directed the project. JK: designed and built the robot, developed methodology, performed the testing and validation, and wrote the original draft of the manuscript. NP: developed model, wrote code, performed analysis, validated the model, and contributed to writing and editing of the manuscript. MT and WX: provided directions and revised and edited the manuscript. JK, NP, WX, and MT: analyzed the data and interpreted and discussed the results.

Supplementary material

Supporting Information is available from the journal online repository or from the corresponding author upon request.

Appendix A. Supporting information

Supplementary data associated with this article can be found in the online version at doi:10.1016/j.sna.2024.115835.

References

[1] C. Laschi, B. Mazzolai, M. Cianchetti, Soft robotics: technologies and systems pushing the boundaries of robot abilities, Sci. Robot. vol. 1 (1) (Dec. 2016) eaah3690, https://doi.org/10.1126/scirobotics.aah3690.
[2] C. Zhang, P. Zhu, Y. Lin, Z. Jiao, J. Zou, Modular soft robotics: modular units, connection mechanisms, and applications, Adv. Intell. Syst. vol. 2 (6) (Jun. 2020) 1900166, https://doi.org/10.1002/aisy.201900166.
[3] M.A. Karimi, V. Alizadehyazdi, H.M. Jaeger, M. Spenko, A self-reconfigurable variable-stiffness soft robot based on boundary-constrained modular units, IEEE Trans. Robot. vol. 38 (2) (Apr. 2022) 810–821, https://doi.org/10.1109/TRO.2021.3106830.
[4] R. Das, S.P.M. Babu, F. Visentin, S. Palagi, B. Mazzolai, An earthworm-like modular soft robot for locomotion in multi-terrain environments, Sci. Rep. vol. 13 (1) (Jan. 2023) 1571, https://doi.org/10.1038/s41598-023-28873-w.
[5] J. Hughes, U. Culha, F. Giardina, F. Guenther, A. Rosendo, F. Iida, Soft Manipulators and grippers: a review, Front. Robot. AI vol. 3 (2016) [Online]. Available: https://www.frontiersin.org/articles/10.3389/frobt.2016.00069.
[6] F. Stella, J. Hughes, D. Rus, C. Della Santina, Prescribing cartesian stiffness of soft Robots by co-optimization of shape and segment-level stiffness, Soft Robot. vol. 10 (Jan. 2023), https://doi.org/10.1089/soro.2022.0025.
[7] D.S. Shah, J.P. Powers, L.G. Tilton, S. Kriegman, J. Bongard, R. Kramer-Bottiglio, A soft robot that adapts to environments through shape change, Nat. Mach. Intell. vol. 3 (1) (Jan. 2021) 51–59, https://doi.org/10.1038/s42256-020-00263-1.
[8] C.D. Onal, D. Rus, A modular approach to soft robots, 2012 4th IEEE RAS EMBS Int. Conf. Biomed. Robot. Biomechatronics (BioRob) (Jun. 2012) 1038–1045, https://doi.org/10.1109/BioRob.2012.6290290.
[9] K.M. Digumarti, A.T. Conn, J. Rossiter, EuMoBot: replicating euglenoid movement in a soft robot, J. R. Soc. Interface vol. 15 (148) (Nov. 2018) 20180301, https://doi.org/10.1098/rsif.2018.0301.
[10] L. Qin, X. Liang, H. Huang, C.K. Chui, R.C.-H. Yeow, J. Zhu, A versatile soft crawling robot with rapid locomotion, Soft Robot. vol. 6 (4) (Aug. 2019) 455–467, https://doi.org/10.1089/soro.2018.0124.
[11] M.A. Robertson, J. Paik, New soft robots really suck: vacuum-powered systems empower diverse capabilities, Sci. Robot. vol. 2 (9) (Aug. 2017) eaan6357, https://doi.org/10.1126/scirobotics.aan6357.
[12] Y. Sun, et al., Soft Mobile Robots: a review of soft robotic locomotion modes, Curr. Robot. Rep. vol. 2 (4) (Dec. 2021) 371–397, https://doi.org/10.1007/s43154-021-00070-5.
[13] I. Must, E. Sinibaldi, B. Mazzolai, A variable-stiffness tendril-like soft robot based on reversible osmotic actuation, Nat. Commun. vol. 10 (1) (Jan. 2019) 344, https://doi.org/10.1038/s41467-018-08173-y.
[14] K.J. McDonald, L. Kinnicutt, A.M. Moran, T. Ranzani, Modulation of magnetorheological fluid flow in soft robots using electropermanent magnets, IEEE Robot. Autom. Lett. vol. 7 (2) (Apr. 2022) 3914–3921, https://doi.org/10.1109/LRA.2022.3147873.
[15] S.W. Kwok, et al., Magnetic assembly of soft robots with hard components, Adv. Funct. Mater. vol. 24 (15) (Apr. 2014) 2180–2187, https://doi.org/10.1002/adfm.201303047.
[16] J. Knospler, W. Xue, M. Trkov, Reconfigurable modular soft robots with modulating stiffness and versatile task capabilities, Smart Mater. Struct. vol. 33 (065040) (2024).
[17] S.L. Brunton, J.L. Proctor, J.N. Kutz, Discovering governing equations from data by sparse identification of nonlinear dynamical systems, Proc. Natl. Acad. Sci. - PNAS vol. 113 (15) (2016) 3932–3937, https://doi.org/10.1073/pnas.1517384113.
[18] F. Ilievski, A.D. Mazzeo, R.F. Shepherd, X. Chen, G.M. Whitesides, Soft Robotics for Chemists, Angew. Chem. Int. Ed. vol. 50 (8) (Feb. 2011) 1890–1895, https://doi.org/10.1002/anie.201006464.
[19] Z. Liu, F. Wang, S. Liu, Y. Tian, D. Zhang, Modeling and analysis of soft pneumatic network bending actuators, IEEE/ASME Trans. Mechatron. vol. 26 (4) (2021) 2195–2203, https://doi.org/10.1109/TMECH.2020.3034640.
[20] A. Ghadami, B.I. Epureanu, Data-driven prediction in dynamical systems: recent developments, 20210213–20210213, in: Philosophical transactions of the Royal Society of London. Series A: Mathematical, physical, and engineering sciences, vol. 380, The Royal Society, 2022.
[21] D. Bruder, C.D. Remy, R. Vasudevan, Nonlinear System Identification of Soft Robot Dynamics Using Koopman Operator Theory. 2019 International Conference on Robotics and Automation (ICRA), IEEE, 2019, pp. 6244–6250, https://doi.org/10.1109/ICRA.2019.8793766.
[22] D. Bruder, X. Fu, R.B. Gillespie, C.D. Remy, R. Vasudevan, Data-driven control of soft robots using koopman operator theory, IEEE Trans. Robot. vol. 37 (3) (2021) 948–961, https://doi.org/10.1109/TRO.2020.3038693.
[23] D. Papageorgiou, G. Þ Sigurðardóttir, E. Falotico, S. Tolu, Sliding-mode control of a soft robot based on data-driven sparse identification, Control Eng. Pract. vol. 144 (2024) 105836, https://doi.org/10.1016/j.conengprac.2023.105836.
[24] D. Bhattacharya, R. Hashem, L.K. Cheng, W. Xu, Nonlinear model predictive control of a robotic soft esophagus, IEEE Trans. Ind. Electron. (1982) vol. 69 (10) (2022) 10363–10373, https://doi.org/10.1109/TIE.2021.3121755.
[25] S.L. Brunton, J.L. Proctor, J.N. Kutz, Sparse identification of nonlinear dynamics with, Control (SINDYc), *IFAC-Pap.* (2016) 710–715, https://doi.org/10.1016/j.ifacol.2016.10.249.

[26] B. de Silva, K. Champion, M. Quade, J.-C. Loiseau, J. Kutz, S. Brunton, PySINDy: a python package for the sparse identification of nonlinear dynamical systems from data, 2104–2104, J. Open Source Softw. vol. 5 (49) (2020), https://doi.org/10.21105/joss.02104.
[27] A. Kaptanoglu, et al., PySINDy: a comprehensive python package for robust sparse system identification, J. Open Source Softw. vol. 7 (69) (2022) 3994, https://doi.org/10.21105/joss.03994.
[28] E. Kaiser, J.N. Kutz, S.L. Brunton, Sparse identification of nonlinear dynamics for model predictive control in the low-data limit, 20180335–20180335, Proc. R. Soc. A, Math., Phys., Eng. Sci. vol. 474 (2219) (2018), https://doi.org/10.1098/rspa.2018.0335.
[29] L.H. Blumenschein, N.S. Usevitch, B.H. Do, E.W. Hawkes, A.M. Okamura, Helical actuation on a soft inflated robot body, 2018 IEEE Int. Conf. Soft Robot. (RoboSoft) (Apr. 2018) 245–252, https://doi.org/10.1109/ROBOSOFT.2018.8404927.
[30] C.D. Onal, D. Rus, Autonomous undulatory serpentine locomotion utilizing body dynamics of a fluidic soft robot, Bioinspiration Biomim. vol. 8 (2) (Mar. 2013) 026003, https://doi.org/10.1088/1748-3182/8/2/026003.
[31] M. Luo, et al., Motion planning and iterative learning control of a modular soft robotic snake, Front. Robot. AI vol. 7 (2020). ⟨https://www.frontiersin.org/articles/10.3389/frobt.2020.599242⟩ ([Online]. Available).
[32] X. Sui, H. Cai, D. Bie, Y. Zhang, J. Zhao, Y. Zhu, Automatic generation of locomotion patterns for soft modular reconfigurable robots, Appl. Sci. vol. 10 (1) (2020), https://doi.org/10.3390/app10010294.
[33] S. Robla-Gómez, V.M. Becerra, J.R. Llata, E. González-Sarabia, C. Torre-Ferrero, J. Pérez-Oria, Working together: a review on safe human-robot collaboration in industrial environments, IEEE Access vol. 5 (2017) 26754–26773, https://doi.org/10.1109/ACCESS.2017.2773127.
[34] Y. Zou, D. Kim, P. Norman, J. Espinosa, J.-C. Wang, G.S. Virk, Towards robot modularity — A review of international modularity standardization for service robots, Robot. Auton. Syst. vol. 148 (Feb. 2022) 103943, https://doi.org/10.1016/j.robot.2021.103943.
[35] K. Gilpin, A. Knaian, D. Rus, Robot pebbles: One centimeter modules for programmable matter through self-disassembly (May), 2010 IEEE Int. Conf. Robot. Autom. (2010) 2485–2492, https://doi.org/10.1109/ROBOT.2010.5509817.
[36] S. Li, et al., Scaling Up soft robotics: a meter-scale, modular, and reconfigurable soft robotic system, Soft Robot. vol. 9 (2) (Apr. 2022) 324–336, https://doi.org/10.1089/soro.2020.0123.

Joshua Knospler received his B.S. in Mechanical Engineering from Rowan University, Glassboro, NJ, USA. He is currently working towards his Masters thesis at Rowan University. His research interests include mechanical design, modular and reconfigurable robots, and soft robotics.

Nicholas Pagliocca received his B.S. and M.S. in Mechanical Engineering from Rowan University, Glassboro, NJ, USA in 2020 and 2022, respectively. His master's thesis research focused on the design and control of modular soft robotic actuators with architected structures. His research interests include functional materials, metamaterials, sensors and actuators, system identification, and soft robotics.

Wei Xue received the B.S. and M.S. degrees in Electrical Engineering from Shandong University, Jinan, China, in 1997 and 2000, respectively, and the Ph.D. degree in Mechanical Engineering from the University of Minnesota, Twin Cities, MN, USA, in 2007. He is currently an Associate Professor in Department of Mechanical Engineering at Rowan University, Glassboro, NJ, USA. His research interests include functional materials, sensors and actuators, and flexible electronics for medical applications.

Mitja Trkov received a B.S. degree in Mechanical Engineering from the University of Ljubljana, Slovenia in 2007 and the Ph.D. degree in Mechanical and Aerospace Engineering from Rutgers University, Piscataway, NJ, USA, in 2016. He was a postdoctoral research fellow in Mechanical Engineering with the University of Utah, Salt Lake City, UT, USA. His research interests include human-machine interactions, robotics, system dynamics and control, mechatronics, and biomechanics with applications in biomedical engineering, autonomous systems, and civil engineering.